Using 2-Aminopurine Fluorescence To Detect Bacteriophage T4 DNA Polymerase−DNA Complexes That Are Important for Primer Extension and Proofreading Reactions†

Chithra Hariharan‡ and Linda J. Reha-Krantz*

Department of Biological Sciences, University of Alberta, Edmonton, Alberta T6G 2E9, Canada

Received July 25, 2005; Revised Manuscript Received October 7, 2005

ABSTRACT: The fluorescence of the base analogue 2-aminopurine (2AP) was used to probe bacteriophage T4 DNA polymerase-induced conformational changes in the template strand produced during the nucleotide incorporation and proofreading reactions. 2AP fluorescence in DNA is quenched by 2AP interactions with neighboring bases, but T4 DNA polymerase binding to DNA substrates labeled with 2AP in the templating position produces large increases in fluorescence intensity. Fluorescence lifetime studies were performed to characterize the fluorescent complexes. Three fluorescence lifetime components were observed for unbound DNA substrates as reported previously, but T4 DNA polymerase binding modulated the amplitudes of these components and created a new, highly fluorescent 10.5 ns component. Experimental evidence for correlation of fluorescence lifetimes with functionally distinct complexes was obtained by forming complexes under different reaction conditions. T4 DNA polymerase complexes were formed with DNA substrates with matched and mismatched primer ends and with A+T- or G+C-rich primer-terminal regions. dTTP was added to binary complexes to form ternary DNA polymerase−DNA-nucleotide complexes. The effect of temperature on complex formation was studied, and complexes were formed with proofreading-defective T4 DNA polymerases. Complexes characterized by the 10.5 ns lifetime were demonstrated to be formed at the crossroads of the primer-extension and proofreading pathways.

DNA polymerases form many different complexes with DNA during the course of the nucleotide incorporation and proofreading reactions. Several structures have been captured in X-ray crystallographic studies: binary complexes with the primer-end bound in the polymerase or exonuclease active center (for example, see refs *1*−*3*), ternary enzyme−DNA-dNTP complexes (for example, see refs *4* and *5*), and complexes formed with damaged DNAs (*6*−*8*) or DNA substrates with mismatches at the primer ends (*9*). While crystallographic snapshots of DNA polymerase complexes provide important information about DNA polymerase−DNA interactions, DNA replication is a dynamic process (reviewed in ref *10*), and thus, studies in solution are required to fully understand all aspects of DNA replication.

One experimental approach that can provide information about DNA polymerase dynamics and structure is fluorescence spectroscopy. For example, DNA can be labeled extrinsically by tethering a fluorophore to one of the DNA bases as was done with studies of interactions between the Klenow fragment and a DNA substrate labeled with a dansyl fluorophore; both polymerase and exonuclease binding modes were detected (*11*). More intimate enzyme−DNA interactions within the polymerase and exonuclease active centers of DNA polymerases can be observed with the fluorescent base analogue 2-aminopurine (2AP).[1] Because 2AP is an analogue of adenine that forms a Watson−Crick base pair with thymine (T) (*12*), DNA polymerases can incorporate the 2AP nucleotide (*13*, *14*) and replicate 2AP-labeled template strands (*15*−*17*). The bacteriophage T4 DNA polymerase, however, discriminates in the use of the 2AP nucleotide (d2APTP), prefers dATP for nucleotide incorporation (*17*, *18*), and actively removes much of the d2APMP that is incorporated by exonucleolytic proofreading (*18*, *19*). Thus, 2AP is a useful base analogue to study fidelity mechanisms employed by phage T4 and other DNA polymerases.

Unlike the natural bases, however, 2AP is fluorescent, which can be exploited to probe DNA polymerase interactions with DNA. 2AP fluorescence is strongly quenched within strands of RNA (*20*) and DNA (*19*, *21*), primarily by interactions between 2AP and the flanking bases (*22*), but if protein binding perturbs these interactions, large increases in fluorescence intensity are observed. For example, a 40-fold increase in 2AP fluorescence intensity is detected for

† This research was supported by grant 14300 from the Canadian Institutes of Health Research. L.R.-K. is a Scientist of the Alberta Heritage Foundation for Medical Research.

* To whom correspondence should be addressed. Telephone: 780-492-5383. Fax: 780-492-9234. E-mail: linda.reha-krantz@ualberta.ca.

‡ Current address: National Chemical Laboratory−Pune, Dr. Homi Bhabha Road, Pashan, Maharastra, 411 008, India.

[1] Abbreviations: 2AP, 2-aminopurine; dAPTP, 2-aminopurine 2′-deoxyribonucleoside 5′-triphosphate; dAPMP, 2-aminopurine 2′-deoxyribonucleoside 5′-monophosphate; dATP, 2′-deoxyadenosine 5′-triphosphate; dTTP, 2′-deoxythymidine 5′-triphosphate; dNTP, 2′-deoxynucleoside 5′-triphosphate; T4-exo⁻, exonuclease-deficient D112A/E114A-DNA polymerase; L412M-exo⁻, exonuclease and proofreading-deficient D112A/E114A/L412M-DNA polymerase; G255S-DNA polymerase, proofreading-defective DNA polymerase; *τ*, fluorescence lifetime.

10.1021/bi051462y CCC: $30.25 © 2005 American Chemical Society
Published on Web 11/10/2005

T4 DNA polymerase complexes formed with DNA substrates labeled with 2AP at the primer terminus compared to the unbound DNA substrate (*19*). Fluorescence lifetime studies revealed that the large increase in fluorescence intensity observed for these complexes is caused by formation of a highly fluorescent component with a lifetime (τ) of about 9.4 ns (*23*). Existence of the 9.4 ns lifetime component was correlated with formation of complexes in which 2AP at the primer end is bound in the exonuclease active center (*23*, *24*) with base unstacking produced by a phenylalanine residue wedged between the two terminal bases (*2*, *6*).

T4 DNA polymerase also forms highly fluorescent complexes with DNA substrates labeled with 2AP in the +1 position in the template strand (Figure 1A) (*15*−*17*). A 20-fold increase in fluorescence intensity is detected when the exonuclease-deficient D112A/E114A-T4 DNA polymerase (T4-exo$^-$) binds DNA labeled with 2AP at the +1 position (Figure 1A; *16*). Much smaller increases in fluorescence intensity are detected for 2AP placed at other positions in the template strand, which indicates that only the base in the +1 position is subject to extensive enzyme-induced base unstacking (*16*, *23*). The large increase in 2AP fluorescence intensity produced by T4-exo$^-$ binding was correlated with forming polymerase complexes, because the large increase in fluorescence intensity was not observed for complexes formed with DNA substrates containing a terminal mismatch, which favors the formation of exonuclease complexes (*16*). Two mechanisms for base unstacking in the template strand have been observed in DNA polymerase structures that could explain the increase in 2AP fluorescence: base flipping and strand bending. Base flipping was detected for a structure of the large fragment of the *Thermus aquaticus* DNA polymerase (Klentaq1) (*3*), and strand bending to various degrees has been observed in structures of several DNA polymerases (for examples, see refs *4*−*9*).

The DNA sequence of the primer-terminal region affects the level of fluorescence intensity observed for binary complexes formed with DNA labeled at the +1 position with 2AP; fluorescence intensity is much higher for complexes formed with DNA substrates in which the primer-terminal region has a high content of AT rather than GC base pairs (*16*). We proposed that the A+T- or G+C-richness of the primer-terminal region affects partitioning between two distinct polymerase complexes. Because increased proofreading is detected for A+T-rich DNA substrates (*18*, *19*, *24*, *25*), the highly fluorescent binary complexes formed with A+T-rich DNA substrates were proposed to be complexes formed at the crossroads of the primer extension and proofreading reactions (*16*). On the other hand, because G+C-richness reduces proofreading (*18*, *19*, *24*, *25*), the less fluorescent complexes formed with G+C-rich DNAs were proposed to be nucleotide preinsertion complexes that are formed in preparation to bind the next incoming nucleotide.

Fluorescence lifetime experiments were performed to test these proposals. The fluorescence decay curves for T4 DNA polymerase binary complexes resolved into multiple fluorescence lifetime components, which indicates the formation of several complexes with 2AP in different environments. Evidence for the existence of multiple fluorescent species and correlation of fluorescence lifetimes with complexes of defined function were obtained by forming T4 DNA polymerase complexes under a variety of experimental conditions

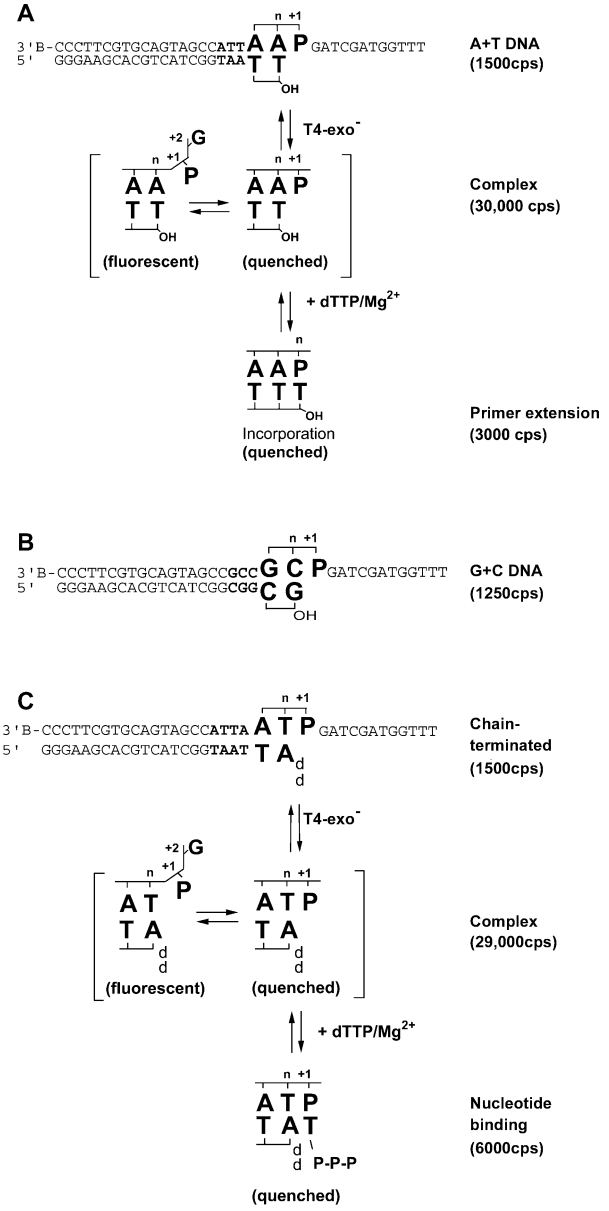

FIGURE 1: Interactions of the exonuclease-deficient D112A/E114A-T4 DNA polymerase (T4-exo$^-$) with DNA substrates labeled with 2AP in the +1 position in the template strand. 2AP is illustrated as a **P**. (A) Interactions of T4-exo$^-$ with an A+T-rich DNA substrate. T4-exo$^-$ (400 nM) was mixed with 200 nM A+T-rich DNA to form fluorescent binary complexes as described in the Materials and Methods. A variety of complexes are formed as discussed in the text; hypothetical structures with 2AP unstacked and stacked are illustrated. The addition of dTTP and Mg^{2+} results in the incorporation of dTMP opposite template 2AP and a quench in 2AP fluorescence. Fluorescence intensities are given for unbound DNA substrates, binary complexes, and complexes formed after dTMP is incorporated. (B) One of the G+C-rich DNA substrates used in this study. (C) Interactions of T4-exo$^-$ with a chain-terminated A+T-rich DNA substrate. Binary complexes were formed as described in A. dTTP was added (150 μM) in the presence of 10 mM Mg^{2+}; formation of the ternary enzyme−DNA-dTTP complex quenches 2AP fluorescence.

that are known to favor either the formation of polymerase or exonuclease complexes. Mutant T4 DNA polymerases with defects in the proofreading reaction were also employed. These findings provide a basis for interpretation of changes in 2AP fluorescence intensity observed during the course of the nucleotide incorporation and proofreading reactions catalyzed by the T4 DNA polymerase (*15*−*17*) and for

learning new insights into how DNA polymerases assess the primer terminus as a substrate for continued primer elongation or for proofreading.

MATERIALS AND METHODS

DNA Polymerases. Expression, purification, and characterization of the wild-type and mutant T4 DNA polymerases were described previously (*24*, *26*−*28*).

DNA Substrates. The DNA substrates have been described (*16*, *17*). Two of the DNA substrates, an A+T-rich and a G+C-rich DNA substrate, are illustrated in parts A and B of Figure 1, respectively. These and other DNA substrates used in this paper vary only in the primer-terminal region, which is indicated in bold in the DNA substrates illustrated in Figure 1. The 2AP phosphoramidite was purchased from Glen Research. The 3′ terminus of the template strand was protected from DNA polymerase binding (to direct enzyme binding to the primer terminus) by a biotin attachment (BiotinTEG-CPG, Glen Research). The primer and template DNAs were annealed in buffer containing HEPES (pH 7.6) and 50 mM NaCl with a 20% excess of the primer strand to ensure complete hybridization of the template strand.

Fluorescence Intensity Experiments. Fluorescence emission data for 2AP-labeled DNAs and DNA polymerase complexes were obtained with a Photon Technology International (PTI) scanning spectrofluorometer. Samples were excited at 315 nm to minimize excitation of tryptophan residues in the T4 DNA polymerase and fluorescence emission was monitored at 368 nm. A 2 nm band-pass was used for both the excitation and emission monochromators. Solutions of complexes were formed with 200 nM to 1 μM 2AP-labeled DNA and DNA polymerase at 1.5- or 2-fold the concentration of DNA in buffer containing 25 mM HEPES (pH 7.6), 50 mM NaCl, 1 mM DTT, and 0.5 mM EDTA. For dTTP titration experiments, the dideoxy chain-terminated DNA substrate illustrated in Figure 1C was used. $MgCl_2$ (10 mM), which is essential for dTTP binding (*16*), and dTTP at the indicated concentrations were added to the solution of binary complexes. Note that, while Mg^{2+} was required for dTTP binding, the presence or absence of Mg^{2+} for other complexes did not affect fluorescence intensities or lifetimes. All experiments were preformed at 20 °C, except where indicated.

Fluorescence Lifetime Measurements. Solutions of DNA (2−4 μM) or complexes (200 nM to 1 μM) in buffer [25 mM HEPES (pH 7.6), 50 mM NaCl, 1 mM DTT, and 0.5 mM EDTA] were excited at 315 nm using the frequency-doubled output from a pulsed dye laser (PTI). The PTI LaserStrobe Lifetime System is capable of resolving lifetimes as short as 100−200 ps. Fluorescence emission was monitored at 368 nm, with a band-pass of 6−8 nm. A stroboscopic optical box car method was used for the determination of fluorescence lifetimes (*29*). The instrument response function was determined by scattering the excitation light with a dilute solution of nondairy coffee creamer. Decay curves were averaged from at least seven acquisitions. All experiments were performed at 20 °C, except where indicated.

The fluorescence decay curves were analyzed by a reconvolution procedure using a nonlinear regression program supplied by PTI (*29*). Fluorescence intensity decay curves were fit to a sum of exponentials

$$I(t) = \sum_{i=1}^{n} \alpha_i e^{-t/\tau_i}$$

where τ_i values are the fluorescence lifetimes and the pre-exponentials α_i values are the amplitudes of each component. Individual fits for each decay curve were obtained by first determining the minimal number of exponential components required to adequately represent the data. Good curve fits for DNA and complexes were obtained with three or four lifetime components as indicated but not with distribution fits. The χ^2 values of good curve fits (provided by the PTI software program) ranged between 0.96 and 1.2, and random distributions of residuals were observed. The reported errors come from assessment of confidence limits.

A global-fitting procedure that links fluorescence lifetimes, also supplied by PTI, was used to determine if T4 DNA polymerase complexes formed under different experimental conditions shared a common set of lifetime components. For many experiments, the lifetime values obtained by fitting individual curves and by global analysis did not vary significantly. The results of global analyses are presented in Figures 3−5, and the results of individual curve fits are given in Supplemental Tables 1−4 in the Supporting Information.

Because more than one exponential term was required to fit the decay curves in our studies, number-averaged fluorescence lifetimes were computed according to the equation

$$\langle \tau_{num} \rangle = \sum_{i=1}^{n} \alpha_i \tau / \sum_{i=1}^{n} \alpha_i \quad (2)$$

The value τ_{num} is proportional to the quantum yield in the absence of static quenching.

RESULTS

Fluorescence Lifetimes of the 2AP Base, 2AP in DNA, and 2AP-Labeled DNA Bound by T4 DNA Polymerase. Time-resolved fluorescence decays for 2AP in different environments are shown in Figure 2. While the decay curve for the 2AP base was monoexponential with a fluorescence lifetime (τ) of about 12.3 ns, the decay curves for the unbound A+T- and G+C-rich 2AP-labeled DNA substrates (illustrated in parts A and B of Figure 1) and for T4-exo$^-$ binary complexes formed with these DNAs were more complex (Table 1). Three lifetime components were required to obtain good fits for the fluorescence decays for the unbound DNAs and T4-exo$^-$ complexes formed with the G+C-rich DNA. Attempts to fit the fluorescence decays with fewer lifetimes were unsuccessful as judged by χ^2 values and by the distribution of residuals (Figure 2). Previous fluorescence lifetime studies of DNA labeled with 2AP in various positions also resolved three or four lifetimes, which indicates that the natural flexibility of DNA in solution places 2AP in different environments (*21*, *30*). Subtle differences in the fluorescence lifetimes for the unbound A+T- and G+C-rich DNAs were observed, which was expected because DNA sequence effects on 2AP fluorescence have been reported (*21*, *30*−*32*).

The decay curves for complexes formed with T4-exo$^-$ and the A+T-rich DNA substrate could be fit with either three lifetime components or four, if the longest lifetime component was fixed. For three component curve fits, a single lifetime of about 9−10 ns replaced the 8.3 and 10.5 ns

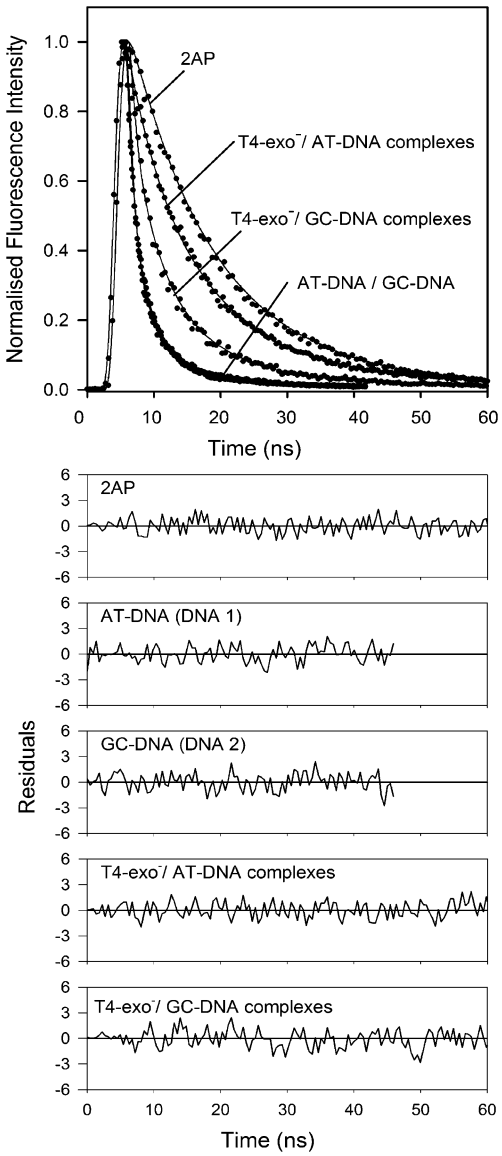

FIGURE 2: Time-resolved fluorescence decays for 2AP in different environments. Decay curves for the 2AP base, binary complexes formed with T4-exo$^-$ and A+T- and G+C-rich DNA substrates, and unbound DNAs are shown. The smooth lines are the best-fit curves; residuals for each fit are shown in the lower panels. The fluorescence lifetimes and pre-exponential factors are listed in Table 1.

components obtained for curve fits with four components (Table 1). While it is normally not possible to recover decay components that differ by just 20% (8.3 and 10.5 ns) from a single decay curve, observations from several experiments reported below provide evidence for the formation of complexes characterized by the 10.5 ns lifetime and, thus, justify the curve fits with four components.

The major lifetime component detected for the unbound 2AP-labeled DNAs was 0.4 ns, which is much less than the 12.3 ns lifetime measured for the 2AP base (Table 1) and demonstrates that 2AP fluorescence in DNA is quenched, as reported (*20*, *21*). T4-exo$^-$ binding, however, increased the fluorescence of 2AP in DNA by 20-fold for the A+T-rich DNA and by 12-fold for the G+C-rich DNA compared to the unbound DNAs (Table 1). For complexes formed with the A+T-rich DNA, the increase in 2AP fluorescence intensity was caused primarily by an abundant 10.5 ns fluorescence lifetime component that was not detected for the unbound DNAs or for complexes formed with the G+C-rich DNA (Table 1). The 0.7 ns component was the most abundant species detected for complexes formed with the G+C-rich DNA (Table 1).

When multiple fluorescent components are resolved from fluorescence decay curves, it is necessary to obtain corroborating evidence for their existence, which we provide in the following experiments. Because different experimental conditions were used to favor the formation of polymerase or exonuclease complexes, changes in fluorescence intensity are predicted to be mainly due to changes in ground-state populations.

dTTP Titrations of T4-exo$^-$ Binary Complexes Formed with Chain-Terminated DNA Substrates: Formation of Nucleotide Insertion Complexes. We observed previously that addition of dTTP/Mg^{2+} to binary complexes formed with T4-exo$^-$ and the chain-terminated A+T-rich DNA substrate illustrated in Figure 1C quenches 2AP fluorescence in a concentration-dependent manner and allows determination of the K_d for dTTP binding, which is about 34 μM (*16*, *17*). Fluorescence lifetime studies were performed to learn more about the quenching mechanism. Because the addition of dTTP forces the formation of ternary enzyme−DNA-dTTP complexes (Figure 1C) and, thus, redistributes ground-state populations, the decrease in fluorescence intensity is predicted to be caused by formation of less fluorescent ternary complexes at the expense of more fluorescent binary complexes. This was observed (Figure 3A). As the concentration of dTTP increased, amplitudes of the 10.5 and 3.2 ns components decreased, while the amplitude of the shortest lifetime component, 0.8 ns, increased (Figure 3A). The amplitude of the 8.3 ns component first increased and then decreased as the concentration of dTTP increased.

The decay curves for each dTTP concentration were first analyzed individually (Supplemental Table 1 in the Supporting Information), but satisfactory fits were also obtained by global analysis (Figure 3A). The satisfactory fits for global analysis are consistent with the model that the addition of dTTP redistributes the ground-state populations of complexes without altering the lifetimes of the individual components, which is further supported by the linearity of the Stern−Volmer plot (Figure 3B).

A dTTP titration was also done with complexes formed with T4-exo$^-$ and the chain-terminated G+C-rich DNA (Supplemental Table 1 in the Supporting Information). These decay curves were fit with three exponential components because the 10.5 ns species was not detected for complexes formed with the G+C-rich DNA. As the concentration of dTTP increased, amplitudes of the two longest lifetime components, about 8.3 and 3.2 ns, decreased, while the amplitude of the shortest lifetime components (0.6−0.7 ns) increased. For T4-exo$^-$ complexes formed with either the chain-terminated A+T- or G+C-rich DNAs, dTTP drove the formation of primarily a single species (≥90%), which was characterized by the shortest lifetime detected for complexes, 0.6−0.8 ns. Thus, fluorescent complexes characterized by lifetimes of about 0.6−0.8 ns are correlated with the formation of ternary complexes with dTTP bound opposite template 2AP (Figure 1C).

Formation of Exonuclease Complexes with Mismatched DNA Substrates. Although the A+T-rich DNA substrates

Table 1: Fluorescence Lifetimes of the 2AP Base, 2AP-Labeled DNA, and Binary Complexes Formed with 2AP-Labeled DNA and T4-exo^{-}[a]

		fluorescence lifetimes					
state	relative intensity	τ_1 (±0.2) (ns)	τ_2 (±0.5) (ns)	τ_3 (±0.5) (ns)	τ_4 (±0.5) (ns)	$\langle\tau_{num}\rangle$ (ns)	χ^2
2AP	47	12.3 [1.00]				12.3	1.11
AT-DNA (DNA 1)	1	0.4 [0.84]	3.2 [0.12]	8.3 [0.04]		1.1	1.03
GC-DNA (DNA 2)	1	0.4 [0.84]	2.9 [0.14]	8.2 [0.02]		0.9	0.97
T4-exo^{-}/AT-DNA complexes	20	0.8 [0.20]	3.2 [0.15]	8.3 [0.10]	10.5 [0.55]	7.2	1.02
T4-exo^{-}/GC-DNA complexes	12	0.7 [0.65]	3.5 [0.10]	8.1 [0.25]		2.8	1.19

[a] Fluorescence lifetimes were determined as described in the Materials and Methods for the indicated molecules and complexes; 2AP is at 200 nM in all cases. The decay curves and fits are shown in Figure 2. DNA 1 and DNA 2 are the A+T- and G+C-rich DNAs illustrated in parts A and B of Figure 1. Errors in fluorescence lifetime (τ) are indicated in parentheses. The pre-exponential factors (amplitudes) are indicated in brackets; errors for amplitudes are ±0.05. Relative fluorescence intensities of the complexes are with respect to the unbound DNAs. The relative intensity of 2AP is with respect to the unbound A+T-rich DNA.

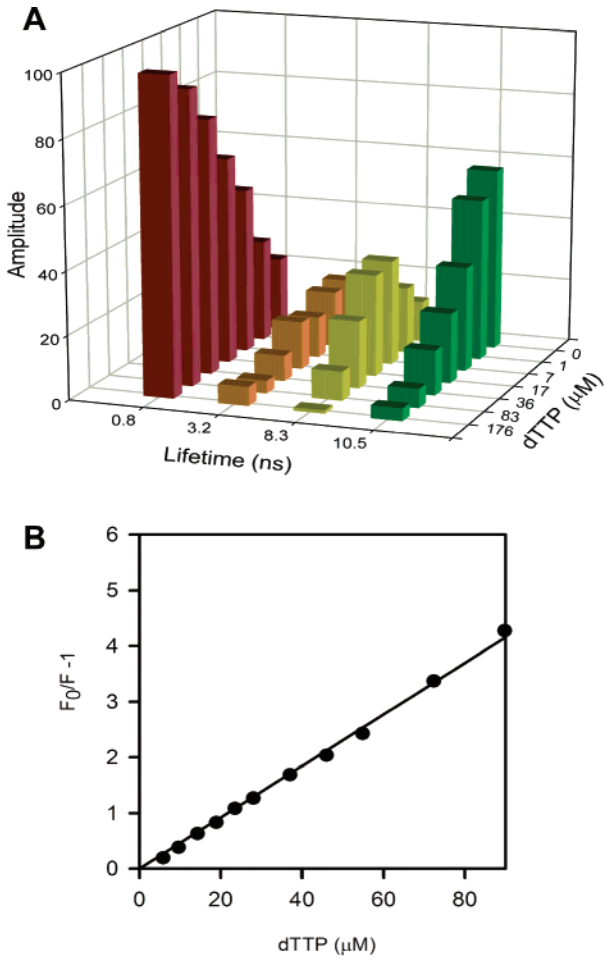

FIGURE 3: Formation of ternary T4-exo^{-}−DNA-dTTP complexes as a function of the dTTP concentration. (A) T4-exo^{-} (1.5 μM) was mixed with 1 μM chain-terminated A+T-rich DNA in buffer containing 10 mM Mg^{2+}. The addition of dTTP quenched 2AP fluorescence and shifted the distribution of fluorescence lifetime components as indicated. A common set of four lifetimes was obtained by global analysis. The fluorescence lifetimes, amplitudes, and average lifetime values for individual curve fits are given in Supplemental Table 1 in the Supporting Information for the A+T-rich DNA illustrated in Figure 1C and for similar experiments with a G+C-rich DNA substrate. (B) Stern−Volmer plot for the observed quench in 2AP fluorescence produced by dTTP binding to T4-exo^{-} complexes.

are correctly base-paired, one or more of the lifetime components detected in the complexes could be due to the formation of exonuclease complexes because T4 DNA polymerase degrades duplex DNA in the absence of nucleotides (*33*), particularly A+T-rich DNAs (*34*). To enhance the formation of exonuclease complexes, binary complexes were formed with preformed mismatched DNA substrates with 2AP in the +1 position (Table 2). The mismatched DNA substrates resemble the A+T-rich DNA illustrated in Figure 1A except for the mismatches (Table 2). For complexes formed with the doubly mismatched DNA substrate with two terminal A−G mismatches, 75% of the complexes formed with the wild-type T4 DNA polymerase were characterized by a 2.8 ns lifetime. A 3.0 ns component was the predominant species formed with T4-exo^{-}, but the amplitude was less (60%), which was expected because T4-exo^{-} has reduced ability to form exonuclease complexes (*19*).

We attempted to drive the formation of complexes with a single fluorescence lifetime component by increasing the temperature to 40 °C because heating increases strand separation, which assists the formation of exonuclease complexes. However, only small increases in the amplitude of the 2.8−3.0 ns component were observed to produce maximum amplitudes of 77 and 68% for the wild-type and T4-exo^{-} polymerases, respectively (Table 2). Thus, the 2.8−3.0 ns component appears to identify exonuclease complexes, but because the amplitude of this component reached only 77%, exonuclease complexes may be a dynamic mixture of complexes with different fluorescence lifetimes and/or small amounts of other types of complexes are also present.

To address these possibilities, the local environment of 2AP in the single-stranded region of the template strand in exonuclease complexes was probed by comparing fluorescence lifetimes for 2AP placed in the +1 position with 2AP placed in the "*n*" (base pairing) or +2 positions (Table 2). Fluorescence lifetimes and amplitudes for exonuclease complexes with 2AP in the *n* and +2 positions were very similar to the distribution of fluorescent components observed for exonuclease complexes formed with 2AP in the +1 position (Table 2), which suggests that the local environments of 2AP in the *n*, +1, and +2 positions are similar. Because the 2.8−3 ns lifetime is longer than the predominant lifetime of the unbound DNA substrate, 0.4 ns (Table 1), the span of single-stranded template DNA from the *n* to the +2 position appears to have a conformation that allows at least transient base unstacking.

Exonuclease complexes are formed preferentially with DNAs with 2AP at the 3′ terminus of the primer strand opposite template T, which indicates that T4 DNA polymerase regards the terminal 2AP-T base pair as a mismatch (*19*, *23*, *24*). We repeated these experiments but with 2AP in the template strand and T at the 3′ terminus of the primer strand (Table 2). Again, T4 DNA polymerase appeared to

Table 2: Binary Complexes Formed with Mismatched DNA Substrates[a]

DNA	mismatch	enzyme	fluorescence lifetimes τ_1 (±0.2) (ns)	τ_2 (±0.5) (ns)	τ_3 (±0.5) (ns)	$\langle\tau_{num}\rangle$ (ns)
ATTAA**P**G	2 mismatches	WT-T4	0.8 [0.13]	2.8 [0.75]	8.5 [0.12]	3.2
TAA**GG**	**P** in +1 position	20 °C				
ATTAA**P**G	2 mismatches	WT-T4	1.2 [0.15]	2.8 [0.77]	8.2 [0.08]	3.0
TAA**GG**	**P** in +1 position	40 °C				
ATTAA**P**G	2 mismatches	T4-exo$^-$	0.8 [0.28]	3.0 [0.60]	8.8 [0.12]	3.1
TAA**GG**	**P** in +1 position	20 °C				
ATTAA**P**G	2 mismatches	T4-exo$^-$	1.2 [0.23]	2.8 [0.68]	8.8 [0.09]	3.0
TAA**GG**	**P** in +1 position	40 °C				
ATTA**P**AG	2 mismatches	WT-T4	0.8 [0.16]	3.0 [0.77]	8.5 [0.07]	3.0
TAA**GG**	**P** in "*n*" position	20 °C				
ATTAAT**P**	2 mismatches	WT-T4	0.9 [0.22]	3.0 [0.72]	8.2 [0.06]	2.9
TAA**GG**	**P** in +2 position	20 °C				
ATTAA**P**G	1 mismatch	WT-T4	0.8 [0.24]	2.8 [0.62]	8.5 [0.14]	3.1
TAATT**T**	**P** in "*n*" position	20 °C				

[a] Binary complexes were formed with DNA substrates containing mismatched primer termini, which resemble the A+T-rich DNA illustrated in Figure 1A except for the sequences shown above. 2-Aminopurine (**P**) and the mismatches are highlighted in bold. Fluorescence lifetimes were determined as described in the Materials and Methods. Errors in fluorescence lifetime (τ) are indicated in parentheses. The pre-exponential factors (amplitudes) are indicated in brackets; errors for amplitudes are ±0.05.

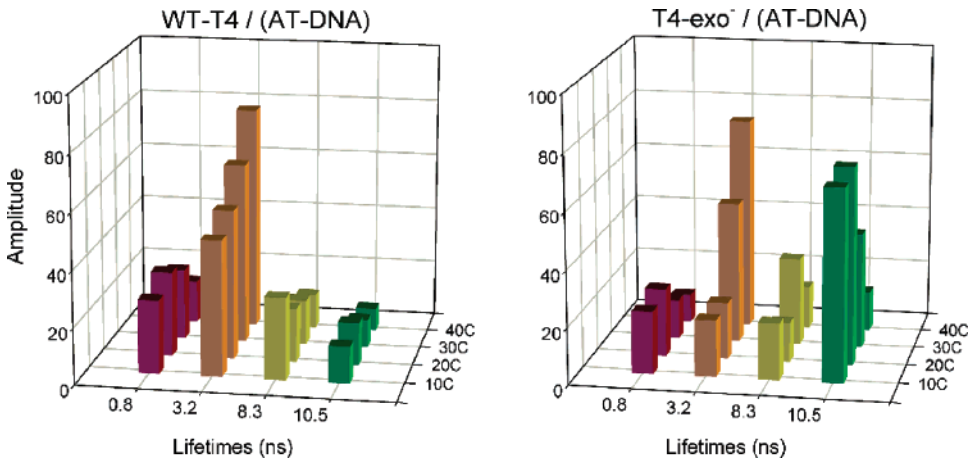

FIGURE 4: Temperature effect on the distribution of fluorescence components. Wild type or T4-exo$^-$ (400 nM) was mixed with 200 nM A+T-rich DNA to form fluorescent binary complexes as described in the Materials and Methods. Heating increased the amplitude of the 3.2 ns component for complexes formed with both DNA polymerases. A common set of four lifetimes was obtained by global analysis. The fluorescence lifetimes, amplitudes, and average lifetime values for individual curve fits are given in Supplemental Table 2 in the Supporting Information for complexes formed with wild-type T4 DNA polymerase and in Supplemental Table 3 in the Supporting Information for complexes formed with T4-exo$^-$.

form primarily exonuclease complexes because the 2.8 ns component was the most abundant species.

Heating Binary Complexes Formed with Matched DNA Substrates Increases the Formation of Exonuclease Complexes and the 3.2 ns Component. Because heating increases T4 DNA polymerase proofreading of matched DNA substrates (*34*), presumably by increasing the fraying of the primer ends, heating binary complexes formed at low temperature is expected to shift the distribution of complexes in favor of more exonuclease complexes. For complexes formed with the wild-type T4 DNA polymerase and the matched A+T-rich DNA substrate, heating complexes from 10 to 40 °C increased the amplitude of the 3.2 ns component from 44 to 75%, while the amplitude of the 10.5 ns component remained essentially constant (7−8%); decreases in the amplitudes of the 0.8 and 8.3 ns components offset the increase observed for the formation of the 3.2 ns component (Figure 4). The decay curves were fit individually (Supplemental Table 2 in the Supporting Information), but satisfactory fits were also obtained by global analysis (Figure 4), which suggests that heating redistributes the ground-state populations in favor of species with a lifetime of about 3.2 ns. Note that, while fraying may occur at the ends of the DNA substrates at 40 °C, this temperature is well below the melting temperature of the A+T-rich duplex substrate, which is about 57 °C. The T_m for the G+C-rich duplex is about 67 °C. Thus, enzyme−DNA complexes are formed with duplex DNAs under these experimental conditions.

For complexes formed with T4-exo$^-$, only 15% of the binary complexes formed at low temperature (10−20 °C) were characterized by the 3.2 ns lifetime compared to 44−48% of the complexes formed with wild-type T4 DNA polymerase (global analysis in Figure 4; individual fits in Supplemental Table 3 in the Supporting Information). The reduced ability of T4-exo$^-$ to form complexes at 10−20 °C characterized by the 3.2 ns lifetime with the matched A+T-rich DNA was offset by increased formation of complexes characterized by the 10.5 ns component (Figure 4). Heating T4-exo$^-$ complexes to 40 °C, however, shifted the distribution of complexes; the amplitude of the 3.2 ns component increased from 15 to 72%, while the amplitude of the 10.5 ns component decreased from about 55 to 10%. At 40 °C,

Table 3: Binary Complexes Formed with T4-exo$^-$ and A+T- and G+C-rich DNA Substrates[a]

DNA		fluorescence lifetimes				
		τ_1 (±0.2) (ns)	τ_2 (±0.5) (ns)	τ_3 (±0.5) (ns)	τ_4 (±0.5) (ns)	$\langle\tau_{num}\rangle$ (ns)
3	ATTAAT**P**G TAATTA	0.9 [0.22]	3.2 [0.13]	8.0 [0.13]	10.2 [0.52]	7.0
4	ATTAAC**P**G TAATTG	1.0 [0.39]	3.2 [0.12]	8.3 [0.23]	10.7 [0.26]	5.5
5	GCCGCT**P**G CGGCGA	0.8 [0.37]	3.6 [0.12]	8.3 [0.43]	10.0 [0.08]	5.1
6	CGCCGG**P**G GCGGCC	0.8 [0.86]	3.2 [0.10]	8.0 [0.04]		1.3

[a] Binary complexes were formed with six DNA substrates that varied only in the primer-terminal region. The prototype A+T- and G+C-rich DNAs 1 and 2 are illustrated in parts A and B of Figure 1, and the fluorescence lifetimes determined for these DNAs are presented in Table 1. The DNA sequence of the primer-terminal regions for DNAs 3−6 are given; the remainder of the DNA sequences are identical to DNAs 1 and 2. 2AP is illustrated as a **P**. Fluorescence lifetimes were determined as described in the Materials and Methods. Errors in fluorescence lifetime (τ) are indicated in parentheses. The pre-exponential factors (amplitudes) are indicated in brackets; errors for amplitudes are ±0.05. Relative fluorescence intensities are with respect to the intensities measured for the unbound DNA substrates. The χ^2 values for the fits varied between 0.96 and 1.20.

there was essentially no difference in the distribution of lifetime components detected for binary complexes formed with the wild-type or T4-exo$^-$ polymerases (Figure 4), which indicates that increased temperature assists T4-exo$^-$ in forming the 3.2 ns component at the expense of the 10.5 ns component.

Complexes were also formed with the G+C-rich DNA substrate (Figure 1B) and the wild-type and T4-exo$^-$ polymerases. The matched G+C-rich DNA substrate was expected to favor the formation of polymerase complexes because G+C-richness reduces proofreading (*19*, *25*). In keeping with this prediction, the shortest lifetime component detected, 0.7−0.9 ns, was the predominant component detected for complexes formed with both DNA polymerases at 10 °C, 64 and 70%, respectively, for wild type and T4-exo$^-$ (Supplemental Tables 2 and 3 in the Supporting Information). Only 10−13% of the complexes were characterized by the lifetime associated with forming exonuclease complexes, about 3.0−3.5 ns. Heating the complexes formed with both DNA polymerases to 40 °C, however, increased the amplitude of the 3.0−3.5 ns component to 60−65% while decreasing the amplitude of the 0.7−0.9 ns component to about 25% (Supplemental Tables 2 and 3 in the Supporting Information). Thus, while the formation of apparent polymerase complexes characterized by the 0.7−0.9 ns lifetime is favored at 20 °C, the increased temperature appears to destabilize the G+C-rich DNA to promote the increased formation of complexes characterized by the 3.0−3.5 ns lifetime.

While the increased temperature has a well-established role in assisting the formation of exonuclease complexes (*18*, *34*), heating may have other effects on 2AP fluorescence, namely, to quench 2AP fluorescence dynamically by increasing collisions between neighboring bases. We observed, however, that 2AP fluorescence in unbound DNAs increased slightly at 55 °C compared to 20 °C (data not shown), which suggests that the major effect of temperature on 2AP fluorescence is to facilitate base unstacking. Thus, the temperature effects observed on 2AP fluorescence in T4 DNA polymerase complexes appear to be caused primarily by shifts in the distribution of ground-state populations of complexes rather than by heat-induced nonradiative decay.

Effect of A+T- and G+C-Richness of DNA Substrates on the Formation of Complexes Characterized by the 10.5 ns Lifetime Component. Fluorescence lifetimes were determined for several binary complexes that were formed with T4-exo$^-$ and a variety of DNA substrates that differed in the number and orientation of AT and GC base pairs in the primer-terminal region (Tables 1 and 3). Complexes were formed with three primarily A+T-rich and three primarily G+C-rich DNA substrates. Fluorescence lifetimes detected for complexes formed with the A+T-rich DNA 1 (Figure 1A) were very similar to complexes formed with the A+T-rich DNA 3, which has an additional AT base pair compared to DNA 1, and 2AP is adjacent to a 3′ T instead of a 3′ A (Tables 1 and 3). DNA 4 differs from DNA 3 by having a single CG base pair at the primer terminus. The addition of a terminal CG base pair to the otherwise A+T-rich primer-terminal region reduced the amplitude of the longest lifetime component and increased the amplitudes of the 8.3 ns and shortest lifetime components (Table 3).

While the 10.5 ns component was not detected for complexes formed with the G+C-rich DNA 2 (Table 1), the addition of a single terminal TA base pair to the otherwise G+C-rich DNA (DNA 5) produced complexes in which a 10.0 ns species was a minor component (Table 3). The 8.3 ns component was the most abundant species detected for complexes formed with DNA 5 (Table 3), while the 0.7 ns component was the most abundant species observed for complexes formed with the fully G+C-rich DNA 2 (Table 1). Reversing the orientation of the terminal CG base pair in DNA 2 to GC in DNA 6 produced complexes with the lowest fluorescence intensity and the highest concentration of the shortest lifetime species (Table 3). The low fluorescence intensity of complexes formed with DNA 6 suggests that G may form an unusual complex with 2AP, which will be studied in future experiments.

Complexes were also formed with two additional DNA substrates that resembled the A+T-rich DNA 3 and the G+C-rich DNA 5, except that the 5′ G adjacent to 2AP in the template strand was replaced by a 5′ C. These experiments were performed to determine if the 5′ G adjacent to 2AP affected fluorescence. No differences were observed for complexes formed with the 5′ C versions of DNAs 3 and 5 (data not shown).

Formation of Binary Complexes with Mutant T4 DNA Polymerases Defective in Proofreading. As discussed above, more of the 10.5 ns component was detected for complexes formed at 20 °C with the A+T-rich DNA and T4-exo$^-$ than with the wild-type T4 DNA polymerase (Figure 4). The wild-

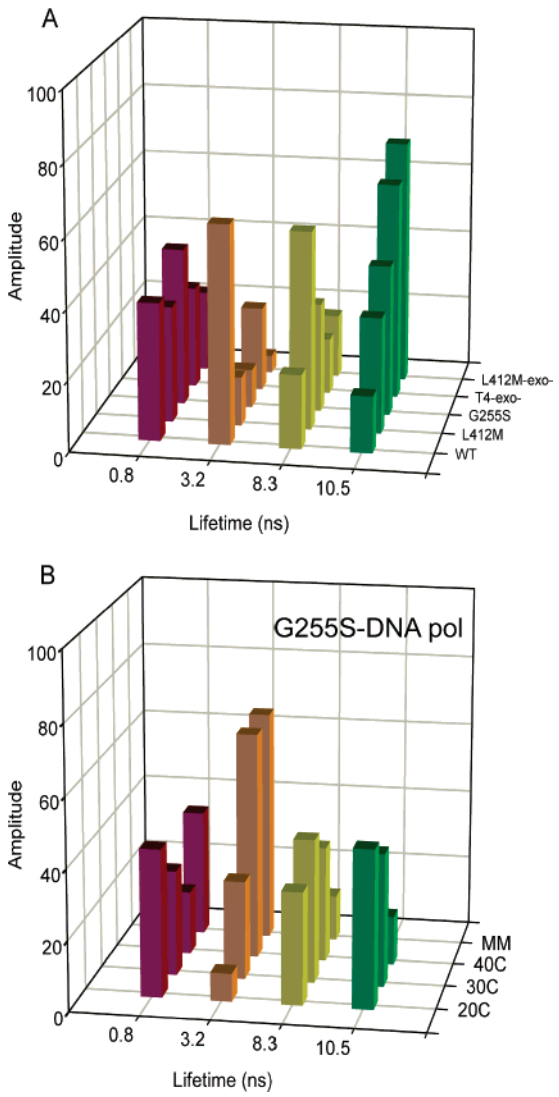

FIGURE 5: Formation of binary complexes with proofreading-defective DNA polymerases. Mutant DNA polymerases (400 nM) were mixed with 200 nM A+T-rich DNA to form fluorescent binary complexes as described in the Materials and Methods. (A) Reduced ability to proofread increases formation of complexes characterized by the 10.5 ns lifetime and decreases formation of complexes characterized by the 3.2 ns lifetime. (B) Increased temperature and preformed mismatches at the primer terminus assist the G255S-DNA polymerase in forming complexes characterized by the 3.2 ns lifetime. A common set of four lifetimes was obtained by global analysis. The fluorescence lifetimes, amplitudes, and average lifetime values for individual curve fits are given in Supplemental Table 4 in the Supporting Information.

type T4 DNA polymerase instead formed more of the 3.2 ns component, which is correlated with formation of exonuclease complexes (Figure 4). Thus, the D112A/E114A amino acid substitutions in the exonuclease active center of T4-exo$^-$ affect partitioning between fluorescent species by increasing the formation of complexes characterized by the 10.5 ns lifetime while decreasing formation of exonuclease complexes.

Additional mutant T4 DNA polymerases with defects in exonucleolytic proofreading were examined for their ability to form the 10.5 and 3.2 ns components (global fits in Figure 5A; individual fits in Supplementary Table 4 in the Supporting Information). The L412M- and G255S-DNA polymerases were discovered by genetic selection methods that identified mutant DNA polymerases with the reduced ability to proofread (*35*). Both the L412M- and G255S-DNA polymerases have a reduced ability to form exonuclease complexes (*24*, *28*, *35*, *36*); thus, both mutant DNA polymerases were predicted to have a reduced ability to form the 3.2 ns component, which was observed (Figure 5A). The decreased ability to form complexes characterized by the 3.2 ns lifetime was accompanied by the increased ability to form complexes characterized by the 10.5 ns lifetime (Figure 5A). The combination of the D112A/E114A and L412M substitutions to produce L412M-exo$^-$ created a mutant DNA polymerase that was even more deficient in forming the 3.2 ns component and more proficient in forming the 10.5 ns component than the singly mutant DNA polymerases (Figure 5A). The reduced amplitude of the 3.2 ns component in complexes formed with the proofreading-defective mutant DNA polymerases provides additional evidence that the 3.2 ns component is a signature for the formation of exonuclease complexes. In addition, because the reduced ability to form the 3.2 ns component is linked to the increased formation of the 10.5 ns component, the 10.5 ns component appears to be formed when the formation of exonuclease complexes is hindered.

To further check that formation of complexes characterized by the 10.5 ns lifetime was due to the hindered formation of exonuclease complexes characterized by the 3.2 ns lifetime, additional studies were done with the G255S-DNA polymerase. In previous studies, we demonstrated that the G255S-DNA polymerase cannot efficiently form exonuclease complexes with matched DNA substrates but can form complexes with DNA substrates with two or three terminal mismatches (*24*). While only 6% of complexes formed with the G255S-DNA polymerase and the matched A+T-rich DNA substrate were characterized by the 3.2 ns lifetime, 61% of the complexes formed with the mismatched DNA with two terminal mismatches were apparent exonuclease complexes with the 3.2 ns lifetime (Figure 5B). Heating binary complexes formed with the matched A+T-rich DNA and the G255S-DNA polymerase also increased the formation of complexes characterized by the 3.2 ns lifetime while decreasing complexes characterized by the 10.5 ns lifetime (Figure 5B).

DISCUSSION

T4 DNA polymerase binding to DNA substrates labeled with 2AP in the templating position produces fluorescent binary complexes, but the fluorescence intensity detected for the complexes depends upon experimental conditions. Fluorescence lifetime experiments were performed to characterize the fluorescent complexes. When complexes were formed under conditions that favor the formation of nucleotide incorporation complexes (G+C-rich DNA, ternary complexes with dTTP), a component with a lifetime of about 0.8 ns was the predominant fluorescent species detected (Tables 1 and 3 and Figure 3A). When complexes were formed under conditions that favor the formation of exonuclease complexes (mismatched DNA substrates, at high temperatures), a component with a lifetime of about 3.2 ns was the predominant species (Table 2 and Figure 4). When complexes were formed with A+T-rich DNAs and proofreading-defective DNA polymerases (Figure 5), a component with a lifetime of about 10.5 ns was the predominant species. Because clear trends for the formation of fluorescent species were observed

with increases in dTTP paralleling increases in the amplitude of the 0.8 ns component (Figure 3A), with increases in temperature paralleling increases in the amplitude of the 3.2 ns component (Figure 4), and with increases in proofreading deficiency paralleling increases in the amplitude of the 10.5 ns component (Figure 5), 2AP appears to be in different conformational states in the functionally distinct complexes. This information can be used to track the formation of different T4 DNA polymerase complexes that are formed with 2AP-labeled DNA throughout the course of the nucleotide incorporation and proofreading reactions.

For experiments that begin with the formation of binary complexes in which 2AP is in the +1 position in the template strand (Figure 1A), 2AP is in position to report on several types of DNA polymerase complexes. DNA polymerases could bind the DNA to form complexes in which a nucleotide has just been incorporated, or complexes may be formed in which the DNA polymerase has translocated and is in position to bind the next incoming nucleotide. Alternatively, if the DNA polymerase cannot form stable polymerase complexes, exonuclease complexes may be produced.

A distinctive complex, characterized by a ~10.5 ns lifetime, was formed with T4-exo$^-$ or other proofreading-deficient DNA polymerases and the A+T-rich DNA substrate (Table 1 and Figure 5). Because the 10.5 ns lifetime is similar to the 10.2−10.4 ns lifetimes determined for the 2AP nucleoside in buffer (*21*, *32*), 2AP in these complexes appears to be solvent-exposed and unstacked. Only the base in the +1 position in these complexes appears to be unstacked because the 10.5 ns lifetime component is not detected for 2AP placed at other positions in the template strand (*16*, data not shown). Although we cannot determine from these studies alone if 2AP base unstacking is produced by DNA-polymerase-induced bending of the template strand, flipping of 2AP to an extra helical position, or some other mechanism, base-base interactions on both sides of 2AP are predicted to be substantially relieved in complexes characterized by the 10.5 ns lifetime.

Our working model is that complexes characterized by the 10.5 ns lifetime are complexes that are not committed to nucleotide incorporation or proofreading but instead are formed at the junction of these two pathways. This proposal is supported by experiments in which reaction conditions were altered to "tip the balance" toward the formation of nucleotide incorporation or proofreading complexes. Nucleotide incorporation complexes were produced by the addition of dTTP/Mg^{2+} to binary complexes formed with T4 exo$^-$ and the chain-terminated A+T-rich DNA substrate (Figure 1C). As the dTTP concentration increased, 2AP fluorescence was quenched, which was caused primarily by a decrease in the amplitude of the highly fluorescent 10.5 ns component and a parallel increase in the amplitude of the 0.8 ns component (Figure 3A and Supplemental Table 1 in the Supporting Information). A complex behavior was observed for the 8.3 ns component, which appeared to increase slightly at low concentrations of dTTP and then to decrease with added dTTP (Figure 3A). We speculate that complexes characterized by the 8.3 ns lifetime are nucleotide preinsertion complexes that may resemble preinsertion complexes detected for the T7 RNA polymerase in which the templating base is somewhat unstacked (*37*). The addition of dTTP initially stabilizes the formation of complexes characterized by the 8.3 ns lifetime at the expense of complexes characterized by the 10.5 ns lifetime. The addition of dTTP also increases the formation of complexes characterized by the 0.8 ns lifetime, and at high concentrations of dTTP, the 0.8 ns species predominates. The reduced fluorescence intensity of 2AP in these enzyme−DNA-dTTP complexes is consistent with structural studies of ternary complexes that show close proximity of the template base with the 3′-neighboring base (*4*, *5*), which is predicted to quench 2AP fluorescence by base−base stacking and collisional interactions as described by Rachofsky et al. (*22*).

Mismatched DNA substrates and increased temperature tip the balance in favor of forming exonuclease complexes. At 40 °C, the most abundant binary complex formed with wild type and T4-exo$^-$ with A+T-rich DNA was characterized by the 3.2 ns lifetime (Figure 4), which is also the approximate lifetime of the most abundant complexes formed with mismatched DNAs (Table 2). To form exonuclease complexes, the primer end is separated from the template strand in a reaction that depends upon a β-hairpin structure that appears to act as a wedge between the two strands (*2*, *6*, *24*). A serine substitution for G255 in the loop of the β-hairpin structure in T4 DNA polymerase significantly reduces the rate of formation of exonuclease complexes and, as a consequence, creates a mutator DNA polymerase (*24*, *35*). In a recent structure of an exonuclease complex formed with the T4-related RB69 DNA polymerase (*6*), the 5′-single-stranded region of the template strand and the tip of the loop of the β-hairpin structure are disordered. These observations were interpreted to indicate movement of the template strand and the β hairpin. 2AP fluorescence studies support this proposal because the 2.8−3.0 ns component was the most abundant species detected for 2AP in the *n*, +1, or +2 positions in exonuclease complexes, which suggests that 2AP in all three positions in the template strand share a similar environment (Table 2). Movement in the single-stranded region is expected to reduce base−base interactions transiently, which could be the basis for generating the ~3.2 ns lifetime.

Studies of proofreading-defective DNA polymerases provide additional evidence that the ~3.2 ns lifetime is a signature for the formation of exonuclease complexes and that complexes characterized by the ~10.5 ns lifetime are formed at the junction of the nucleotide incorporation and proofreading pathways. While 42% of the complexes formed with the wild-type T4 DNA polymerase and the A+T-rich DNA substrate illustrated in Figure 1A were characterized by the ~3.2 ns lifetime (Figure 4), only 3−15% of the complexes formed with proofreading-defective DNA polymerases were characterized by the ~3.2 ns lifetime (Figure 5 and Supplemental Table 4 in the Supporting Information). Instead, proofreading-defective DNA polymerases formed complexes characterized by the ~10.5 ns lifetime; the highest amount of this highly fluorescent component was observed for complexes formed with the multiply mutant L412M-exo$^-$ DNA polymerase (Figure 5A).

An important conclusion from these studies is that T4 DNA polymerase can distinguish between DNA substrates with A+T- or G+C-rich primer-terminal regions and form functionally distinct complexes accordingly. Complexes characterized by the ~3.2 ns fluorescence lifetime, apparent exonuclease complexes, are formed preferentially by the

wild-type T4 DNA polymerase with A+T-rich DNAs, and complexes characterized by the ~0.8 ns lifetime, apparent polymerase complexes, are formed with G+C-rich DNAs (Supplemental Table 2 in the Supporting Information). However, if exonuclease complexes cannot be readily formed with the A+T-rich DNA, as is the case for proofreading-defective T4 DNA polymerases, polymerase complexes characterized by the ~0.8 ns lifetime are not formed as a default; instead, complexes characterized by the ~10.5 ns lifetime are formed (Figure 5). Because translocation after nucleotide incorporation does not appear to be needed to form exonuclease complexes (*6*), complexes characterized by the 10.5 ns lifetime may not have translocated to be in position to bind the next incoming nucleotide. If so, then the A+T-richness of the primer-terminal region results in the formation of stalled T4 DNA polymerase complexes. Interestingly, in some structures of the *Bacillus* DNA polymerase I fragment in "stalled" conformations with different mismatched DNAs, the template strand is bent and the base in the +1 position is unstacked (*9*). If the base in the +1 position was 2AP, then a fluorescent complex would be produced. The ability of DNA polymerases to sense instability of the primer-terminal region is predicted to be useful for detecting buried mismatches and DNA polymerases have been reported to do so (*38*, *39*). DNA polymerases may encounter DNA substrates with matched primer ends but with mismatches or strand misalignments in the primer-terminal region. The correction of these errors by exonucleolytic proofreading before primer elongation could be an important contribution to replication fidelity.

In summary, we provide evidence for a novel DNA polymerase complex, characterized by a ~10.5 ns lifetime, which forms at the crossroads of the nucleotide incorporation and proofreading pathways. These studies also provide a starting point to further probe interactions of the T4 DNA polymerase with 2AP-labeled DNA substrates. For example, the mechanisms for how T4 DNA polymerase detects primer instability and for how 2AP fluorescence is quenched within complexes have not yet been determined. In addition, these studies demonstrate that 2AP fluorescence can be used to measure both the dynamics of DNA polymerase interactions with DNA in real time (*15*−*17*) and to correlate changes in 2AP fluorescence with the formation of functionally distinct complexes.

ACKNOWLEDGMENT

We thank Linda B. Bloom, J. B. Alexander Ross, Evaldus Katilius, and Dina Tleugabulova for helpful discussions of the manuscript.

SUPPORTING INFORMATION AVAILABLE

Supplemental Tables 1−4, which provide data for individual curve fits presented as global fits in Figures 3−5. This material is available free of charge via the Internet at http://pubs.acs.org.

REFERENCES

1. Wang, J., Sattar, A. K. M. A., Wang, C. C., Karam, J. D., Konigsberg, W. H., and Steitz, T. A. (1997) Crystal structure of a pol α family replication DNA polymerase from bacteriophage RB69, *Cell 89*, 1087−1099.
2. Shamoo, Y., and Steitz, T. A. (1999) Building a replisome from interacting pieces: Sliding clamp complexed to a peptide from DNA polymerase and a polymerase editing complex, *Cell 99*, 155−166.
3. Li, Y., Korolev, S., and Waksman, G. (1998) Crystal structures of open and closed forms of binary and ternary complexes of *Thermus aquaticus* DNA polymerase I: Structural basis for nucleotide incorporation, *EMBO J. 17*, 7514−7525.
4. Doublié, S., Tabor, S., Long, A., Richardson, C. C., and Ellenberger, T. (1998) Crystal structure of bacteriophage T7 DNA replication complex at 2.2 Å resolution, *Nature 391*, 251−258.
5. Franklin, M. C., Wang, J., and Steitz, T. A. (2001) Structure of the replication complex of a pol α family DNA polymerase, *Cell 105*, 657−667.
6. Hogg, M., Wallace, S. S., and Doublié, S. (2004) Crystallographic snapshots of a replication DNA polymerase encountering an abasic site, *EMBO J. 23*, 1483−1993.
7. Freisinger, E., Grollman, A. P., Miller, H., and Kisker, C. (2004) Lesion (in)tolerance reveals insights in DNA replication fidelity, *EMBO J. 23*, 1494−1505.
8. Hsu, G. W., Ober, M., Carrell, T., and Beese, L. S. (2004) Error-prone replication of oxidatively damaged DNA by a high-fidelity DNA polymerase, *Nature 431*, 217−221.
9. Johnson, S. J., and Beese, L. S. (2004) Structures of mismatch replication errors observed in a DNA polymerase, *Cell 116*, 803−816.
10. Joyce, C. M., and Benkovic, S. J. (2004) DNA polymerase fidelity: Kinetics, structure, and checkpoints, *Biochemistry 43*, 14317−14324.
11. Thompson, E. H., Z., Bailey, M. F., van der Schans, D. J. C., Joyce, C. M., and Millar, D. P. (2002) Determinants of DNA mismatch recognition within the polymerase domain of the Klenow fragment, *Biochemistry 41*, 713−722.
12. Sowers, L. C., Fazakerley, G. V., Eritja, R., Kaplan, B. E., and Goodman, M. F. (1986) Base pairing and mutagenesis: Observation of a protonated base pair between 2-aminopurine and cytosine in an oligonucleotide by proton NMR, *Proc, Natl. Acad. Sci. U.S.A. 83*, 5434−5438.
13. Pless, R. C., Levitt, L. M., and Bessman, M. J. (1981) Nonrandom substitution of 2-aminopurine for adenine during deoxyribonucleic acid synthesis *in vitro*, *Biochemistry 20*, 6235−6244.
14. Bloom, L. B., Otto, M. R., Beechem, J. M., and Goodman, M. F. (1993) Influence of 5′-nearest neighbors on the insertion kinetics of the fluorescent nucleotide analog 2-aminopurine by Klenow fragment, *Biochemistry 32*, 11247−11258.
15. Frey, M. A., Sowers, L. C., Millar, D. P., and Benkovic, S. J. (1995) The nucleotide analog 2-aminopurine as a spectroscopic probe of nucleotide incorporation by the Klenow fragment of *Escherichia coli* polymerase I and bacteriophage T4 DNA polymerase, *Biochemistry 34*, 9185−9192.
16. Mandal, S. S., Fidalgo da Silva, and Reha-Krantz, L. J. (2002) Using 2-aminopurine fluorescence to detect base unstacking in the template strand during nucleotide incorporation by the bacteriophage T4 DNA polymerase, *Biochemistry 41*, 4399−4406.
17. Fidalgo da Silva, E., Mandal, S. S., and Reha-Krantz, L. J. (2002) Using 2-aminopurine fluorescence to measure incorporation of incorrect nucleotides by wild type and mutant bacteriophage T4 DNA polymerases, *J. Biol. Chem. 277*, 40640−40649.
18. Bessman, M. J., and Reha-Krantz, L. J. (1977) Studies on the biochemical basis of spontaneous mutation. V. Effect of temperature on mutation frequency, *J. Mol. Biol. 116*, 115−123.
19. Bloom, L. B., Otto, M. R., Eritja, R., Reha-Krantz, L. J., Goodman, M. F., and Beechem, J. M. (1994) Pre-steady-state kinetic analysis of sequence-dependent nucleotide excision by the 3′-exonuclease activity of bacteriophage T4 DNA polymerase, *Biochemistry 33*, 7576−7586.
20. Ward, D. C., Reich, E., and Stryer, L. (1969) Fluorescence studies of nucleotides and polynucleotides. I. Formycin, 2-aminopurine riboside, 2,6-diaminopurine riboside, and their derivatives. *J. Biol. Chem. 244*, 1228−1237.
21. Guest, C. R., Hochstrasser, R. A., Sowers, L. C., and Millar, D. P. (1991) Dynamics of mismatched base pairs in DNA, *Biochemistry 30*, 3271−3279.
22. Rachofsky, E. L., Osman, R., and Ross, J. B. A. (2001) Probing structure and dynamics of DNA with 2-aminopurine: Effects of local environment on fluorescence, *Biochemistry 40*, 946−956.
23. Beechem, J. M., Otto, M., Bloom, L. B., Eritja, R., Reha-Krantz, L. J., and Goodman, M. F. (1998) Exonuclease-polymerase active site partitioning of primer-template DNA strands and equilibrium

Mg^{2+} binding properties of bacteriophage T4 DNA polymerase, *Biochemistry 37*, 10144−10155.
24. Marquez, L. A., and Reha-Krantz, L. J. (1996) Using 2-aminopurine fluorescence and mutational analysis to demonstrate an active role of bacteriophage T4 DNA polymerase in strand separation required for 3′ → 5′ exonuclease activity, *J. Biol. Chem. 271*, 28903−28911.
25. Petruska, J., and Goodman, M. F. (1985) Influence of neighboring bases on DNA polymerase insertion and proofreading fidelity, *J. Biol. Chem. 260*, 7533−7539.
26. Reha-Krantz, L. J., Nonay, R. L., and Stocki, S. (1993) Bacteriophage T4 DNA polymerase mutations that confer sensitivity to the PP_i analog phosphonoacetic acid, *J. Virol. 67*, 60−66.
27. Reha-Krantz, L. J., and Nonay, R. L. (1993) Genetic and biochemical studies of bacteriophage T4 DNA polymerase 3′ → 5′ exonuclease activity, *J. Biol. Chem. 268*, 27100−27108.
28. Reha-Krantz, L. J., and Nonay, R. L. (1994) Motif A of bacteriophage T4 DNA polymerase: Role in primer extension and DNA replication fidelity, *J. Biol. Chem. 269*, 5635−5643.
29. James, D. R., Siemiarczuk, A., and Ware, W. R. (1992) Stroboscopic optical boxcar technique for the determination of fluorescence lifetimes, *Rev. Sci. Instrum. 63*, 1710−1716.
30. Hochstrasser, R. A., Carver, T. E., Sowers, L. C., and Millar, D. P. (1994) Melting of a DNA helix terminus within the active site of a DNA polymerase, *Biochemistry 33*, 11971−11979.
31. Xu, D. G., and Nordlund, T. M. (2000) Sequence dependence of energy transfer in DNA oligonucleotides, *Biophys. J. 78*, 1042−1058.
32. Rachofsky, E. L., Seibert, E., Stivers, J. T., Osman, R., and Ross, J. B. A. (2001) Conformation and dynamics of abasic sites in DNA investigated by time-resoloved fluorescence of 2-aminopurine, *Biochemistry 40*, 957−967.
33. Clayton, L. K., Goodman, M. F., Branscomb, E. W., and Galas, D. J. (1979) Error induction and correction by mutant and wild-type T4 DNA polymerase. Kinetic error discrimination mechanisms, *J. Biol. Chem. 254*, 1902−1912.
34. Lo, K.-Y., and Bessman, M. J. (1976) An antimutator deoxyribonucleic acid polymerase. II. *In vitro* studies of its temperature sensitivity, *J. Biol. Chem. 251*, 2480−2486.
35. Stocki, S. A., Nonay, R. L., and Reha-Krantz, L. J. (1995) Dynamics of bacteriophage T4 DNA polymerase function: Identification of amino acid residues that affect switching between polymerase and 3′ → 5′ exonuclease activities, *J. Mol. Biol. 254*, 15−28.
36. Baker, R. P., and Reha-Krantz, L. J. (1998) Identification of a transient excision intermediate at the crossroads between DNA polymerase extension and proofreading pathways, *Proc. Natl. Acad. Sci. U.S.A. 95*, 3507−3512.
37. Temiakov, D., Patlan, P., Aniken, M., McAllister, W. T., Yokoyama, S., and Vassylyev, D. G. (2004) Structural basis for substrate selection by T7 RNA polymerase, *Cell 116*, 381−391.
38. Miller, H., and Grollman, A. P. (1997) Kinetics of DNA polymerase I (Klenow fragment exo^-) activity on damaged DNA templates: Effect of proximal and distal template damage on DNA synthesis, *Biochemistry 36*, 15336−15342.
39. Weiss, S. J., and Fisher, P. A. (1992) Interaction of *Drosophila* DNA polymerase α holoenzyme with synthetic template-primers containing mismatched primer bases or propanodeoxyguanosine adducts at various position in template and primer regions, *J. Biol. Chem. 267*, 18520−18526.

BI051462Y